IMPROVED FLEXIBILITY IN MODR USING A SUPERSONIC JET SOURCE: APPLICATIONS TO CO^+ AND CN

M.A. JOHNSON, M.L. ALEXANDER, I. HERTEL ‡ and W.C LINEBERGER

Department of Chemistry, University of Colorado and Joint Institute for Laboratory Astrophysics, University of Colorado and National Bureau of Standards, Boulder, Colorado 80309, USA

Received 12 December 1983; in final form 16 January 1984

Microwave–optical double resonance (MODR) is carried out on the $N = 1 \leftarrow 0$ transitions of CN and CO^+, which are rotationally cooled in a supersonic jet. Large modulations in the probe LIF (≈100%) are observed without optical saturation, demonstrating that short pulse dye lasers may be used in MODR. Hyperfine constants for $^{12}C^{14}N$ in $\tilde{X}\,^2\Sigma^+(v = 2)$ are reported.

1. Introduction

Since its introduction in 1973 [1], microwave–optical double resonance (MODR) has been an effective tool in analyzing molecular spectra [2]. Users of this technique generally employ cw dye lasers [3–5] or microsecond duration pulsed lasers [6] since the production of strong MODR signals requires simultaneous saturation of *both* the optical and microwave transitions. As a result, the broad tunability of high-power Nd : YAG based dye laser systems has not been exploited in MODR spectroscopy. Clearly, however, if such 10 ns pulsed lasers could be employed as the optical probe in MODR, the technique could be expanded as a general means to obtain structural information on radicals and ions, traditionally difficult [7,8] to observe in microwave spectroscopy.

In this letter, we demonstrate the great advantages of supersonic jet cooling in obtaining (MODR) spectra. We observe microwave transitions in the CO^+ ion and CN radical by detecting the changes in the rotational populations due to saturation of the microwave transition. Hence, a non-saturating laser-induced fluorescence (LIF) population probe suffices to observe the effect. Microwave-induced changes in the probe LIF of as much as 120% are observed, indicating that the transitions are easily seen using the jet. As an indication of the sensitivity of this technique, all nine hyperfine components of the $v = 2, N = 1 \leftarrow 0$ transition of the CN ground electronic state were trivially searched and recorded.

An additional advantage of this method lies in the ability to control the linewidth of the microwave transition by varying the extent of power broadening. When searching for a transition, widths of ≈1 MHz are generated by high microwave power, while measurements of the line position can be obtained at lower power, reducing the width to 200 kHz or less.

2. Experimental

The apparatus consists of a pulsed free-jet molecular beam which passes through three interaction regions in the course of the MODR experiment. The species of interest is first created by electron impact. After rotational cooling through further expansion, microwave transitions are induced in a confocal Fabry–Pérot cavity. Finally, further downstream, laser-induced fluorescence serves to determine the rotational state populations.

The supersonic jet is obtained from a pulsed solenoid

‡ 1983–84 JILA Visiting Fellow. Permanent address: Institut für Molekulphysik, Freie Universität Berlin, D-1000 Berlin 33, Federal Republic of Germany.

valve with a 0.5 mm nozzle diameter and 300 μs pulse duration. Neutral precursors of the CO^+ and CN were seeded in helium as described below.

The expanding jet is first crossed by an electron beam to form the radical or ion species to be studied. The ionization/excitation occurs early in the expansion, and the nascent rotational distributions created by electron impact are allowed to cool during expansion before the beam encounters the microwave field The most important parameter in forming transient species in the jet is the distance between the nozzle and the point of interaction with the electron beam. We have found that intense LIF spectra are most readily obtained when a rectangular cross section "ribbon" of electrons (2 mm X 2 cm) is allowed to impinge on the molecular beam, with the long dimension of the rectangle parallel to the nozzle axis. The electron gun (1 mA, 350 V) is manipulated from outside the vacuum, and the electron-beam–nozzle distance is varied to optimize the LIF signal from the lowest energy rotational level.

The microwave excitation occurs 4 cm from the nozzle, where the rotationally inelastic collision frequency in the beam is negligible and most species are in the ground rotational level. Resonant excitation of rotational transitions thus results in a substantial transfer of population among the driven levels The excitation is carried out in a confocal Fabry–Pérot cavity with an 8 cm spacing between two 5 cm mirrors. The purpose of the cavity is to build up the 100 μW of power produced by our 120 GHz source, a frequency-doubled 60 GHz klystron, so that microwave transitions could be easily saturated. The half-width of the resonance for the TEM_{00} $q \approx 60$ mode was measured by detecting the dip in reflected power and was found to be 5 MHz, giving a Q of 24000 and a finesse of 300. The gaussian beam waist in the cavity where the microwaves intersect the molecular beam is calculated to be 0.5 cm, and the circulating power is estimated to be 10 mW. The Zeeman broadening of lines due to the Earth's magnetic field was eliminated with Helmholtz coils.

After microwave excitation, the rotational population distribution of the transient species is interrogated by LIF. The laser (Nd : YAG pumped dye) crosses the molecular beam 1.5 cm below the center of the Fabry–Pérot. Careful imaging of the fluorescence ensures that only those molecules exposed to microwave radiation are probed by LIF. It was also necessary to pulse the electron beam off 20 μs prior to firing the laser to allow the background emission from species excited by electron impact to decay.

2.1. Formation and characterization of rotationally cooled CN and CO^+

The CO^+ and CN species are formed by electron impact on a beam composed of a mixture of helium and either CO or CH_3CN. Stagnation pressure and the percent seed of the neutral precursor in the helium bath gas are important parameters, optimized by trial and error. For CO^+, 20% CO in helium at a stagnation pressure of 2.5 atm gave an intense CO^+ signal with the electron excitation beginning $\approx$1 cm below the nozzle. On the other hand, CN was best generated by passing He at 9 atm through liquid CH_3CN, with the electron excitation beginning at the nozzle.

As was previously observed by Heaven et al. [9], rotational states are readily relaxed, while the nascent vibrational distribution is essentially intact after the expansion. This effect is quite pronounced as seen in the LIF spectrum (microwaves off) presented in fig. 1. Here we see a $\approx$2 K CN rotational distribution superimposed on a 5000 K vibrational distribution! The nascent CN distributions created by the process

$$CH_3CN + e^- \rightarrow CH_3 + CN\ B\,^2\Sigma^+(v,J) + e^-$$

have been reported by Tokue et al. [10], using dispersed fluorescence, with the result that the vibrational

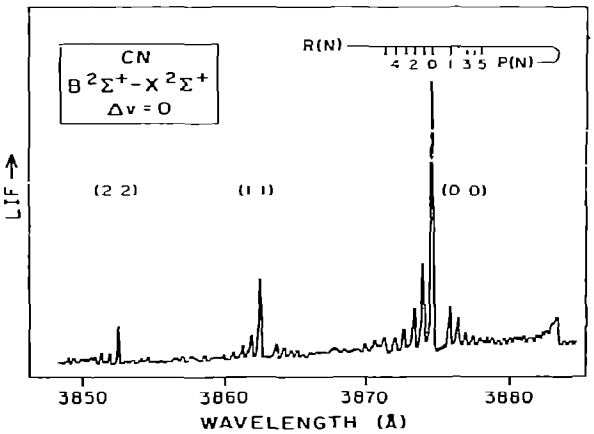

Fig. 1. LIF spectrum of jet-cooled CN, produced by electron impact dissociation of CH_3CN, and expanded in helium at a stagnation pressure of 9 atm.

and rotational distributions are described by effective Boltzmann temperatures of $T_v \approx 7000$ K and $T_R \approx 1200$ K. Clearly, substantial rotational relaxation has occurred in the high-density region of the expansion.

In the case of CO^+, rotational temperatures of 10–20 K were readily achieved, but the population in $v = 1$ was less than 1% of that in $v = 0$. This was somewhat surprising in light of the fact that the population in $v = 1$ formed by electron impact is 10% of that in $v = 0$. It appears likely that this result arises from the rapid, near-resonant charge transfer process [11]

$$CO^+(v = 1) + CO(v = 0) \rightarrow CO(v = 1) + CO^+(v = 0),$$

which serves to deplete the $v = 1$ CO^+ formed by electron impact.

2.2 *Data acquisition: generation of MODR spectra*

MODR spectra are observed by monitoring the LIF from a given rotational line while the microwave frequency is swept through a resonance. Since the rotational transitions are narrow, accurate frequency control is essential if the fullest advantages of rotational spectroscopy are to be attained. In this experiment, two stages of phase-locking are used to stabilize and measure the 120 GHz output. The experiment is controlled by a microcomputer which repetitively steps the 120 GHz frequency at intervals of 200 kHz, collecting the fluorescence from two laser shots at each microwave frequency. The 5 MHz scan is then repeated until adequate signal-to-noise is achieved (typically 50 scans taking a total of 5 min). Calibration of the 120 GHz microwave frequency was carried out by detecting the well-established [12] 113271.202 MHz $J = 1 \leftarrow 0$ absorption in CO, cooled in the jet.

3. Results and discussion

The essential new feature of this study is the use of jet cooling to create a large population difference among the lowest two rotational levels. When such a distribution of rotational levels can be obtained, the jet acts as a state selector for the lowest rotational level, allowing for a large shift in rotational state populations when the system is driven by the microwave field. The advantage of this effect in MODR is that substantial changes in the probe LIF can be induced by saturating the microwave transition. Moreover, the optical probe is not required to saturate the electronic transition on the timescale of the microwave pumping, and 10 ns laser pulses are adequate to observe the effect. This ability to use short pulses actually has substantial implications for the generality of this technique, since non-fluorescence probe methods such as multiphoton ionization [13] for neutrals and photofragmentation for ions [14] will work equally well in detecting the MODR effect.

The magnitude of the MODR signal resulting from jet cooling is strongly sensitive to the temperature as well as the degree of quantum state selectivity in the optical probe. For instance, the LIF probe used here for CN is the B–X $^2\Sigma^+ - ^2\Sigma^+$ band, where neither the spin–rotation doublet nor the nitrogen hyperfine splittings are resolved. The microwave excitation involves only one of these levels, so that all other levels involved in the optical transition contribute background fluorescence. As an example, consider the transition $|vN'J'F'\rangle - |vN''J''F''\rangle$ in CN:

$$|0,1,3/2,5/2\rangle - |0,0,1/2,3/2\rangle.$$

After microwave saturation, the $|M_F| = 1/2$ and $3/2$ magnetic sublevels of both rotational levels will be equally populated due to the $\Delta M_F = 0$ selection rule for linearly polarized microwaves. This MODR signal, ΔI_m, defined by:

$$\Delta I_m = \frac{\text{LIF(microwaves on)} - \text{LIF(microwaves off)}}{\text{LIF(microwaves off)}}$$

is not dependent on optical saturation since the LIF only serves as a population probe. ΔI_m has a temperature dependence:

$$\Delta I_m = \tfrac{1}{2} f [\exp(\pm \Delta E_N / kT) - 1],$$

where the plus or minus sign applies to whether the LIF probes the upper or lower N state, respectively, ΔE_N is the rotational energy difference between $N = 0$ and 1, and T is the rotational temperature. The statistical factor f gives the ratio of the $2F + 1$ sub-levels involved in the microwave transition ($F = \min(F', F'')$) to the total number of lower levels participating in the LIF probe (18 in the case of CN, $N = 1$). For the CN transition discussed above, $f = 4/18$, and with 2.5 K CN such as was found in the LIF scan in fig. 1, we expect a MODR signal $\Delta I_m = 100\%$ when probing $N = 1$.

3.1. CN

Fig. 2 presents a MODR spectrum of the |0,1,3/2, 5/2⟩–|0,0,1/2,3/2⟩ hyperfine transition in the ground vibrational level of jet-cooled CN ‡. Note that the signal-to-noise on this peak is better than 10/1 in this four minute scan! In addition, the magnitude of the effect is a 120% modulation, as expected from the detailed level argument above. The residual line width of 200 kHz fwhm is primarily due to microwave power broadening.

While the spectrum shown in fig. 2 demonstrates the effectiveness of jet cooling in MODR spectroscopy, its observation is somewhat tempered by the fact that the position of this line is well established by previous laboratory observations [15,16]. We therefore have extended our study of the CN molecule to higher vibrational levels, part of whose rotational spectra have very recently been studied in a gas discharge absorption experiment by Skatrud et al. [16]. These authors did not detect the $N = 1 \leftarrow 0$ rotational transitions, however, and our experiment complements their work. As seen in fig. 1, our jet CN source readily lends itself to such a study since higher vibrational levels are significantly populated while the rotational distributions are still cold.

A search for the $N = 1 \leftarrow 0$ transition of $v = 2$ CN was therefore undertaken, and in 3 h, all nine hyperfine components of this transition were found. A representative spectrum from this search is shown in fig 3, showing the nearly degenerate |2,1,3/2,5/2⟩–|2,0,1/2,3/2⟩ and |2,1,3/2,3/2⟩–|2,0,1/2,1/2⟩ transitions. The two-to-one ratio of these lines is a consequence of the fact that twice as many M_F levels are involved in the larger lines' microwave transition (F = 3/2 and 1/2, respectively). The observed line positions are collected in table 1.

‡ Our measured value of 113490.969(18) for this transition agrees well within the error limits with the value of Dixon and Woods [15] (113490.989(11)).

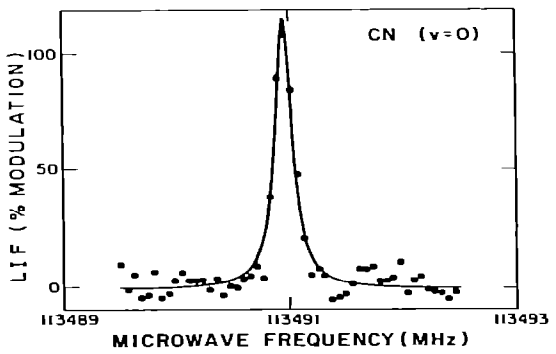

Fig. 2. MODR spectrum of CN (LIF probe on R(1)), taken with reduced microwave power to narrow the line width The microwave stepsize was also reduced to 60 kHz in order to display the line. Solid line is a least-squares fit lorentzian line shape.

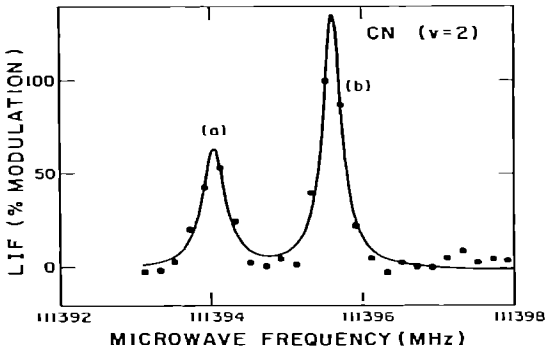

Fig 3. MODR spectrum of CN(v = 2) (LIF probe on R(1)), showing two hyperfine components of the $N = 1 \leftarrow 0$ transition: (a) |2,1,3/2,3/2⟩–|2,0,1/2,1/2⟩, and (b) |2,1,3/2,5/2⟩–|2,0,1/2,3/2⟩. The level notation is defined as |v,N,J,F⟩.

Table 1
Observed hyperfine transition frequencies (MHz) for $^{12}C^{14}N$ in the $X\,^2\Sigma^+(v = 2)$ state

Transition $\lvert N'J'F'\rangle - \lvert N''J''F''\rangle$	Observed [a]	Obs. – calc. [b]
1 1/2 1/2–0 1/2 1/2	111037.824(25)	−0.004
1 1/2 1/2–0 1/2 3/2	111056 036(21)	0 008
1 1/2 3/2–0 1/2 1/2	111084.476(27)	−0.004
1 1/2 3/2–0 1/2 3/2	111102.678(21)	−0.002
1 3/2 3/2–0 1/2 1/2	111394.068(26)	0.012
1 3/2 5/2–0 1/2 3/2	111395.612(20)	−0.014
1 3/2 1/2–0 1/2 1/2	111404.645(23)	0.012
1 3/2 3/2–0 1/2 3/2	111412 258(23)	−0.002
1 3/2 1/2–0 1/2 3/2	111422.834(27)	0.000

a) Numbers in parentheses give one standard deviation from least-squares fits to measured MODR lines plus one estimated standard deviation from calibration error.

b) Calculated values of frequencies from five fitted molecular constants shown in table 2.

Table 2
Molecular constants (MHz) for $^{12}C^{14}N$ in the $X\,^2\Sigma^+(v = 2)$ state

Molecular constant	This work [a]	Skatrud et al. [b]
rotation (B'_2)	55646.722(15)	55646.711 [c]
spin–rotation (γ_2)	212.377 (7)	212.316(29)
magnetic (b_2)	−32.430(8)	−32.489(42)
magnetic (c_2)	60.889(22)	60.930(11)
electric quadrupole (eqQ_2)	−1.018(33)	−1.010(48)

[a] Numbers in parentheses give one standard deviation from least-squares fit to the observed transition frequencies in table 1. In case of B'_2 one standard deviation of the calibration error is added.
[b] Ref. [16]. One standard deviation is given in parentheses.
[c] The B'_2 value is not reported in ref. [16]. Here we compare with 1/2 of the pure rotational energy derived from the Dunham coefficients.

The reduction of these data to molecular constants was done by diagonalizing the hamiltonian given by Dixon and Woods [15], neglecting the interaction between different N levels. The result of a least-squares fit to our nine hyperfine transition frequencies by five molecular constants is shown in table 2, together with the values of Skatrud et al. [16]. While the agreement is generally good, there may be some slight discrepancy in the spin–rotation constant, presumably owing to our observation of a different rotational transition. As seen in table 1, the constants generated by the fit accurately reproduce the measured line positions from this study ‡.

3.2. CO^+

As a final example of the applicability of this technique, we have also obtained the MODR spectrum of the $N = 1 \leftarrow 0$ transition in $X\,^2\Sigma\ CO^+(v = 0)$, observed previously in absorption [17,18] and by optical saturation MODR [6]. Because of the slightly higher rotational temperature obtained in this case, 15 K, compared to 2 5 K in CN, the MODR effect is smaller but, as evident from fig. 4, the $|0, 1, 3/2\rangle - |0, 0, 1/2\rangle$ line is readily observed. In fig. 4, the line is shown both as an increase in LIF from probing with the $R_1(3/2)$ transition and as a decrease in LIF from probing with the $R_1(1/2)$ transition. This behavior is different from the

‡ We have also fit our data to six constants as done by Dixon and Woods [15], which includes the nuclear spin–rotation coupling constant C_I. In spite of some reduction of the variance, the C_I value found, −8.5 ± 10 kHz, was not well defined, and opposite in sign to that found in ref. [15].

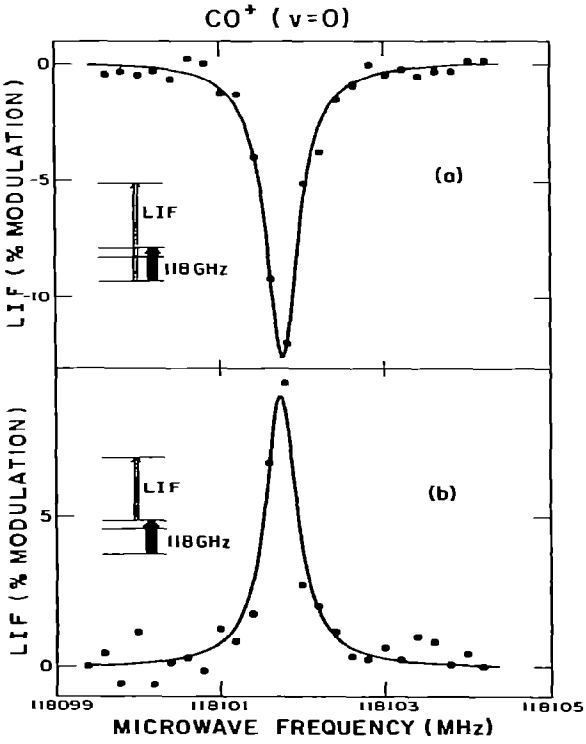

Fig. 4. MODR spectrum of CO^+ $N = 1 \leftarrow 0, |0,1,3/2\rangle - |0,0,1/2\rangle$ spin–rotation component when: (a) the lower level of the microwave transition is probed with LIF of the $R_1(1/2)$ line, and (b) the upper level of the microwave transition is probed with LIF of the $R_1(3/2)$ line. Solid lines are least-squares fitted lorentzian line shapes, constrained to the same width.

Table 3
Transition frequencies for the $^{12}C^{16}O^+$ $X\,^2\Sigma^+(v = 0)$ state; $N = 1 \leftarrow 0$ transition

$J' \leftarrow J''$	Present work	Piltch et al. [17]	Bogey et al. [18]
3/2 1/2	118101.777(26) [a]	118101.886(48)	118101.812(50)
1/2 1/2	117692.315(41) [b]	117692.294(103)	117692.360(30)

[a] Average of fits to six scans. Error is one standard deviation.
[b] Lorentzian fit to one scan. Error is one standard deviation.

MODR spectra reported by Brown et al. [6], who used conventional optical-saturation MODR and observed the microwave transition as a 10% increase in the $R_1(1/2)$ fluorescence. We also note that, in their study, 30% signal-to-noise was achieved only after 10 h of averaging. The magnitude of the effect in this experiment is now 15%, and the spectra shown in fig. 4 result from 10 min averages. Clearly, MODR spectroscopy is qualitatively simpler to execute in the jet. Since there appears to be some discrepancy in the literature as to the exact values of some of the CO^+ transitions, we give our measurements of the $N = 1 \leftarrow 0$ transition in table 3. They agree well within the confidence limits with the data of Bogey et al. [18].

4. Conclusions

Microwave–optical double resonance has been performed on several ground electronic state vibrational levels of CN as well as the ground vibrational level of CO^+, where these species have been rotationally cooled in a supersonic expansion. Large MODR signals are observed by a method which requires the optical probe only as a diagnostic for the rotational distribution, not as an optical pumping source as in previous MODR experiments.

Replacement of the LIF probe with a more general population probe such as multiphoton ionization or multiphoton dissociation seems certain to enhance the generality of MODR for application to a wide variety of transient species.

Acknowledgement

We thank C. Iddings, H. Liebe, K. Evenson, G. Dunn for the loan of microwave equipment. Direction and encouragement from J.J. Gallagher is also gratefully acknowledged. This reaserch was supported by the National Science Foundation under grants PHY82-00805 and CHE83-16628.

References

[1] R.W. Field, A.D. English, T. Tanaka, D.O. Harris and D. Jennings, J. Chem. Phys. 59 (1973) 2191.
[2] G.W. Hills, J. Mol. Spectry. 93 (1982) 395.
[3] W.J. Childs, L.S. Goodman and I. Renhorn, J. Mol. Spectry. 87 (1981) 522.
[4] G.W. Hills, J.M. Cook, R.F. Curl Jr. and F.K. Tittel, J. Chem. Phys. 65 (1976) 823.
[5] S.G. Hansen and B.J. Howard, Chem. Phys. Letters 85 (1982) 249.
[6] R.D. Brown, P.D. Godfrey, D.C. McGilvery and J.G. Crofts, Chem. Phys. Letters 84 (1981) 437.
[7] T.A. Miller, Ann. Rev. Phys. Chem. 27 (1976) 127.
[8] R.J. Saykally and R.C. Woods, Ann. Rev. Phys. Chem. 32 (1981) 403.
[9] M. Heaven, T.A. Miller and V.E. Bondybey, Chem. Phys. Letters 84 (1981) 1.
[10] I. Tokue, T. Urisu and K. Kuchitsu, J. Photochem. 3 (1974/1975) 273.
[11] D.L. Smith and J.H. Futrell, J. Chem. Phys. 59 (1973) 463.
[12] F.J. Lovas and P.H. Krupenie, J. Phys. Chem. Ref. Data 3 (1974) 245.
[13] P.M. Johnson and C.E. Otis, Ann. Rev. Phys. Chem. 32 (1981) 139.
[14] J. Moseley and J. Durup, Ann. Rev. Phys. Chem. 32 (1981) 53.
[15] T.A. Dixon and R.C. Woods, J. Chem. Phys. 67 (1977) 3956.
[16] D.D. Skatrud, F.C. De Lucia, G.A. Blake and K.V.L.N. Sastry, J. Mol. Spectry. 99 (1983) 35.
[17] N.D. Piltch, P.G. Szanto, T.G. Anderson, C.S. Gudeman, T.A. Dixon and R.C. Woods, J. Chem. Phys. 76 (1982) 3385.
[18] M. Bogey, C. Demuynck and J.L. Destombes, J. Chem. Phys. 79 (1983) 4704.